AIAA JOURNAL
Vol. 43, No. 5, May 2005

Boundary Element Method's Treatment of Interfacial Thermal Stresses Between Dissimilar Anisotropic Materials

Y. C. Shiah* and Y. J. Lin†
Feng Chia University, Taichung 40724, Taiwan, Republic of China

One of the most crucial concerns in the use of bonded composites lies in the interfacial thermal stresses developed between dissimilar materials as a result of the mismatch of thermal expansion coefficients. Although the boundary element method (BEM) has been recognized as an efficient computational tool, especially for rapidly varying stresses near the free edge of bonded composites, the study of the interfacial thermal stresses between dissimilar anisotropic materials by BEM still remains unexplored. An intercoupled BEM approach is proposed to investigate the interfacial thermal stresses by transforming the volume integral caused by thermal loading into a series of boundaries ones. Three numerical examples are provided as illustrations of the veracity as well as the applicability of the proposed scheme.

Nomenclature

A_{ij} = complex constants depending on material properties
C_{ij} = geometrical coefficients at the source point
C_0 = heat-source term
K_{ij} = heat-conductivity coefficients of anisotropic materials
n_k = components of the unit outward normal vector along the boundary
P = source point on the boundary
Q = field point on the boundary
Q^* = fundamental solution of the normal temperature gradient
q = field point in the domain
r_{ij} = complex constants depending on material properties
S = boundary surface
T_{ij} = fundamental solution for the traction
t_i = nodal tractions
U_{ij} = fundamental solution for the displacement
u_i = nodal displacements
x_{pi} = coordinates of the source point
β = inclined angle of the outward normal measured from the x_1 axis
γ_{ik} = constant coefficients related to thermal properties of the material
ζ = local coordinates of the field point
Θ = temperature change at the field point
Θ^* = the fundamental solution of the temperature field
μ_i = complex root of the characteristic equation for anisotropic materials
Ω = domain region

I. Introduction

SINCE the early 1960s, structural materials with anisotropic properties have been widely used in numerous commercial, aerospace, and military engineering applications. In recent years, the remarkable progress of industrial technologies has made extremely high demands of anisotropic materials to meet high-level requirements. For various purposes, composites are often constructed by combining two or more anisotropic materials such that the physically or chemically different phases will make possible the high performance. In achieving this high performance, the interaction between constituent materials in the interface is of utmost importance. One of the most crucial concerns in the use of such bonded composites lies in the interfacial thermal stresses developed between dissimilar materials as a result of the mismatch of thermal expansion coefficients, which will cause possible debonding under some circumstance. This has led to increasing attention being paid to the thermoelastic analysis of the interfacial stresses when the bonded structure is subjected to thermal loads.

Although some analytical solutions can be obtained for a few specific problems (e.g., see Suhir[1] and Yin[2]), recourse to numerical methods such as the finite element method (FEM) and the boundary element method (BEM) is usually necessary in general. To this end, the BEM, sometimes also referred to as the boundary-integral-equation (BIE) method, has been recognized as an efficient computational tool for engineering stress analysis, especially for problems with rapidly varying stresses. For complex problems, the BEM has the advantage that less data-storage memories and computation efforts are needed, especially for the thermoelasticity problem that all temperature and its spatial gradients need to be computed for the whole domain by the domain solution techniques. In the BEM, however, only the boundary data are required for the computation. The numerical examples shown in the paper are simply to show the veracity and generality of the proposed scheme. For problems with irregular shapes, however, highly skilled meshing scheme will thus be required by the traditional domain solution techniques like the finite difference method and FEM. Although the behavior of the singular stress field near the free edge has promised excellent accuracy for the use of BEM, the BEM study on the interfacial thermal stresses between dissimilar anisotropic materials subjected to a general thermal field still remain unexplored. The main reason is that thermoelastic effects manifest themselves as additional volume integral terms in BEM for elastostatics when using the direct boundary integral equation formulation. Any numerical BIE formulation that requires the direct evaluation of the volume integral would, however, destroy the notion of the BEM as a computational technique of boundary solution for engineering analysis.

Several schemes have been proposed over the years to resolve this volume integral problem in the BIE analysis of isotropic, elastic bodies when inertial and thermal effects are considered. They include the Monte Carlo and domain fanning approach (e.g., see Camp and Gipson[3]), the particular integral approach (e.g., see Lachat[4] and Deb and Banerjee[5]), and the exact transformation method (ETM) (e.g., see Rizzo and Shippy,[6] Tan,[7] and Danson[8]). Among these schemes, ETM, which exactly transforms the volume integral into a series of integrals over just the boundary, is fundamentally most appealing because it restores the analysis to a purely boundary one without

Received 15 May 2003; revision received 8 December 2004; accepted for publication 12 December 2004.

*Associate Professor, Department of Aerospace and Systems Engineering, No. 100 Wenhwa Road, Seatwen.
†Postgraduate, Department of Aerospace and Systems, No. 100 Wenhwa Road, Seatwen.

the need to make further numerical approximations per se. Although ETM is now widely employed to treat the volume integrals associated with body-force and thermal effects in isotropic elasticity, similar transformations for anisotropic thermoelasticity have not been achieved until very recently when Shiah and Tan[9] successfully transformed the associated volume integral into a series of boundary ones by treating the problem in a sequentially coupled manner. By this approach, the domain for the thermal field must be mapped unto an auxiliary plane, where the associated temperature field in the distorted domain is governed by the standard Laplace's equation. In extending the approach for interior calculations, Shiah and Tan[10] further derived the Somigliana's identity of interior strains under general thermal loads. Despite extensive applications of bonded anisotropic materials in engineering industries, no BEM work has been reported in literature so far to deal with interfacial thermoelastic stresses between dissimilar anisotropic materials under general thermal loads.

In this paper, the ETM is employed to further treat the interfacial problem by the intercoupled way as was done by Shiah and Tan[9] for a single homogeneous domain. For this purpose, the domain needs to be mapped onto the auxiliary plane through a linear coordinate transformation.[11] In the domain mapping process, however, the physical domain becomes distorted in the mapped plane. When a domain consists of several anisotropic regions, for each of which a different set of anisotropic coefficients is involved, the interfaces between dissimilar conjoint materials will, in general, overlap or separate in the mapped plane. To apply the conventional subregioning technique for the thermal field problem in BEM, the compatibility equation considering overlapping/separating interfaces is derived for the present work. To treat the problem in the sequentially coupled way, the computer codes for solving the boundary equations for both problems have been integrated into a single program such that whenever the temperature field data at interior points are required for solving the BIE of thermoelasticity, they can be computed interactively by the BIE for the associated field problem. In contrast with other schemes proposed over the years to treat the thermoelasticity problem, this interactive approach marks the key to solving the sequentially coupled problem by the exactly transformed BIE, yet without any further numerical approximations per se. For illustrations of the veracity as well as the applicability of the proposed scheme, three numerical examples are presented with verification by the analysis of ANSYS6.0, commercial software based on the finite element method.

II. BIE of Thermoelasticity

In the direct formulation of the BEM for an anisotropic solid in two dimensions, the BIE provides an integral relation between the displacements u_i and the tractions t_i on the boundary S of the domain Ω, which is described by

$$C_{ij}u_i(P) + \oint_S u_i(Q)T_{ij}(P, Q)\,\mathrm{d}S = \oint_S t_i(Q)U_{ij}(P, Q)\,\mathrm{d}S + \oint_S \gamma_{ik}n_k\Theta U_{ij}(P, Q)\,\mathrm{d}S - \int_\Omega \gamma_{ik}\Theta_{,k}U_{ij}(P, q)\,\mathrm{d}\Omega \tag{1}$$

The displacement fundamental solution for anisotropic materials U_{ij}, which will be used in the subsequent transformation process for the volume integral, can be written as

$$U_{ij}(P, q) = 2\mathrm{Re}\{r_{i1}A_{j1}\log z(\mu_1) + r_{i2}A_{j2}\log z(\mu_2)\} \tag{2}$$

The generalized variables $z(\mu_i)$, with components denoted by z_1 and z_2 in what follows, are defined by

$$z_i = (x_1 - x_{p1}) + \mu_i(x_2 - x_{p2}) = \zeta_1 + \mu_i\zeta_2 \tag{3}$$

It is apparent that the last term in Eq. (1), a domain integral, would destroy the distinctive feature of BEM as a truly boundary solution computational technique if it is implemented directly. The task now is to analytically transform the domain integral into boundary ones with procedures described as follows.

To treat the thermoelasticity problem in a sequentially coupled manner, we need to start from considering the thermal field problem first. With the assumption of steady-state conditions and the presence of a uniformly distributed heat source in the domain, the temperature change Θ for anisotropic materials must satisfy the heat-conduction equation

$$k_{ij}\Theta_{,ij} = C_0 \tag{4}$$

From thermodynamic considerations and Onsagar's reciprocity relation, these coefficients must satisfy

$$K_{11} > 0, \qquad K_{22} > 0, \qquad K_{12} = K_{21}$$
$$\Delta = K_{11}K_{22} - K_{12}^2 > 0 \tag{5}$$

To facilitate the "volume-to-surface" integral transformation that will be elaborated later, the Euler's equation (4) is transformed into the standard Poisson's equation, that is,

$$\Theta_{,\underline{ii}} = C_1 \tag{6}$$

where the constant C_1 is given by $C_1 = C_0K_{11}/\Delta$; the underline in the indices appearing in Eq. (6) denotes a new coordinate system $(\hat{x}_1, \hat{x}_2)$, defined by the linear transformation

$$[\hat{x}_1 \quad \hat{x}_2]^T = [\boldsymbol{F}(K_{ij})][x_1 \quad x_2]^T$$
$$[x_1 \quad x_2]^T = \left[\boldsymbol{F}^{-1}(K_{ij})\right][\hat{x}_1 \quad \hat{x}_2]^T \tag{7}$$

As is presented in detail by Shiah and Tan,[9] the transformation (or the inverse transformation) matrix in Eq. (7), $[\boldsymbol{F}(K_{ij})]$ [or $\boldsymbol{F}^{-1}(K_{ij})$], has its component elements $[F_{mn}]$ (or $[F^{-1}_{mn}]$), given by

$$\boldsymbol{F} = \begin{pmatrix} \sqrt{\Delta}/K_{11} & 0 \\ -K_{12}/K_{11} & 1 \end{pmatrix}, \qquad \boldsymbol{F}^{-1} = \begin{pmatrix} K_{11}/\sqrt{\Delta} & 0 \\ K_{12}/\sqrt{\Delta} & 1 \end{pmatrix} \tag{8}$$

Figure 1 shows an example of the distortion of a circular domain that is mapped into an oblique ellipse in the transformed coordinate system. With the domain directly mapped onto the auxiliary plane using Eq. (7), the temperature and its gradients at the boundary nodes can therefore be calculated by solving the boundary equation

$$c_i\Theta_i + \int \Theta Q^*\,\mathrm{d}\hat{S} = \int q\Theta^*\,\mathrm{d}\hat{S} \tag{9}$$

Notice that the integration is carried out for the distorted boundary of the mapped domain. The procedures to solve the boundary integral equation for isotropic media have been well established in the BEM literature and therefore will not be elaborated herein. As a postprocess, the solution for the physical domain can, therefore, be obtained by transforming the obtained data back according to the transformation matrix given in Eq. (7). For a complete description of such transformation processes, the reader can refer to the work by Shiah and Tan.[11]

After all field data at boundary nodes, including the temperature and its spatial gradients to the first order, are determined through the process as aforementioned, we can now turn back to the thermoelasticity BIE for anisotropic media. The temperature gradients

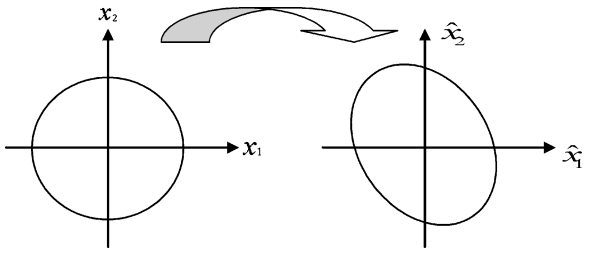

Fig. 1 Domain mapping into the $\hat{x}_i$-coordinate system.

in the original Cartesian coordinate system can then be rewritten in the mapped coordinate system, denoted by the underline in the indices, as follows:

$$\Theta_{,1} = \Theta_{,\underline{1}}\sqrt{\Delta}\big/K_{11} - \Theta_{,\underline{2}}K_{12}/K_{11}, \qquad \Theta_{,2} = \Theta_{,\underline{2}} \tag{10}$$

From these, it can be readily shown that the extra volume integral (VI) in Eq. (3) can be rewritten as

$$\mathrm{VI}_j = -\int_{\hat{\Omega}} \gamma_{i\underline{k}}\Theta_{,\underline{k}}U_{ij}\,\mathrm{d}\hat{\Omega} \tag{11}$$

where $\gamma_{i\underline{k}}$ can be expressed in a matrix form as

$$\gamma_{i\underline{k}} = \begin{pmatrix} \gamma_{11} & \dfrac{-\gamma_{11}K_{12} + \gamma_{12}K_{11}}{\sqrt{K_{11}K_{22} - K_{12}^2}} \\ \gamma_{21} & \dfrac{-\gamma_{21}K_{12} + \gamma_{22}K_{11}}{\sqrt{K_{11}K_{22} - K_{12}^2}} \end{pmatrix} \tag{12}$$

Only the main steps of the exact transformation process will be described here as the complete detail has been presented previously by Shiah and Tan.[9] By applying Green's theorem consecutively together with the auxiliary condition of Eq. (6), it can be shown that the volume integral in Eq. (11) can be analytically transformed into boundary ones as follows:

$$\mathrm{VI}_j = \int_{\hat{S}} [(\gamma_{i\underline{k}}Q_{\underline{ijk},\underline{t}}\Theta - \gamma_{i\underline{k}}Q_{\underline{ijk}}\Theta_{,\underline{t}} + C_1\gamma_{i\underline{k}}R_{\underline{ijkt}})n_{\underline{t}} - \gamma_{i\underline{k}}U_{\underline{ij}}\Theta n_{\underline{k}}]\,\mathrm{d}\hat{S} \tag{13}$$

where the functions $Q_{\underline{ijk}}$, $Q_{\underline{ijk},\underline{t}}$, and $R_{\underline{ijkt}}$ in the integrand are given by

$$Q_{\underline{ijk}} = 2\mathrm{Re}\left\{\frac{r_{i1}A_{j1}\mu_{\underline{k1}}z_{\underline{1}}\log(z_{\underline{1}})}{\left(\mu_{\underline{11}}^2 + \mu_{\underline{21}}^2\right)} + \frac{r_{i2}A_{j2}\mu_{\underline{k2}}z_{\underline{2}}\log(z_{\underline{2}})}{\left(\mu_{\underline{21}}^2 + \mu_{\underline{22}}^2\right)}\right\} \tag{14}$$

$$Q_{\underline{ijk},\underline{t}} = 2\mathrm{Re}\left\{\frac{r_{i1}A_{j1}\mu_{\underline{k1}}\mu_{\underline{t1}}z_{\underline{1}}\log(z_{\underline{1}})}{\left(\mu_{\underline{11}}^2 + \mu_{\underline{21}}^2\right)} + \frac{r_{i2}A_{j2}\mu_{\underline{k2}}\mu_{\underline{t2}}z_{\underline{2}}\log(z_{\underline{2}})}{\left(\mu_{\underline{21}}^2 + \mu_{\underline{22}}^2\right)}\right\} \tag{15}$$

$$R_{\underline{ijkt}} = 2\mathrm{Re}\left\{\frac{r_{i1}A_{j1}\mu_{\underline{k1}}\left(z_{\underline{1}}^2\log(z_{\underline{1}}) - z_{\underline{1}}^2/2\right)}{4\mu_{\underline{t1}}\left(\mu_{\underline{11}}^2 + \mu_{\underline{21}}^2\right)} + \frac{r_{i2}A_{j2}\mu_{\underline{k2}}\left(z_{\underline{2}}^2\log(z_{\underline{2}}) - z_{\underline{2}}^2/2\right)}{4\mu_{\underline{t2}}\left(\mu_{\underline{12}}^2 + \mu_{\underline{22}}^2\right)}\right\} \tag{16}$$

In Eqs. (14–16), $\mu_{\underline{ji}}$ takes the values of the elements of the following matrix:

$$\mu_{\underline{ji}} = \begin{pmatrix} \dfrac{K_{11} + \mu_1 K_{12}}{\sqrt{\Delta}} & \dfrac{K_{11} + \mu_2 K_{12}}{\sqrt{\Delta}} \\ \mu_1 & \mu_2 \end{pmatrix} \tag{17}$$

With the domain integral transformed into boundary ones albeit in the mapped coordinate system, the thermoelasticity BIE for anisotropic materials can now be expressed as follows:

$$C_{ij}u_i(P) + \int_S u_i(Q)T_{ij}(P,Q)\,\mathrm{d}S = \int_S t_i(Q)U_{ij}(P,Q)\,\mathrm{d}S + \int_S \gamma_{ik}n_k\Theta U_{ij}(P,Q)\,\mathrm{d}S + \int_{\hat{S}} [(\gamma_{i\underline{k}}Q_{\underline{ijk},\underline{t}}\Theta - \gamma_{i\underline{k}}Q_{\underline{ijk}}\Theta_{,\underline{t}} + C_1\gamma_{i\underline{k}}R_{\underline{ijkt}})n_{\underline{t}} - \gamma_{i\underline{k}}U_{\underline{ij}}(P,Q)\Theta n_k]\,\mathrm{d}\hat{S} \tag{18}$$

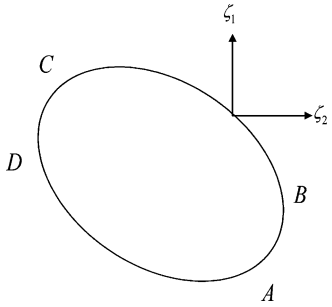

Fig. 2 Simply connected convex domain.

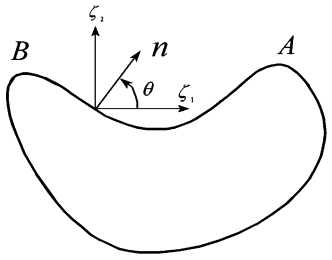

Fig. 3 Simply connected nonconvex domain.

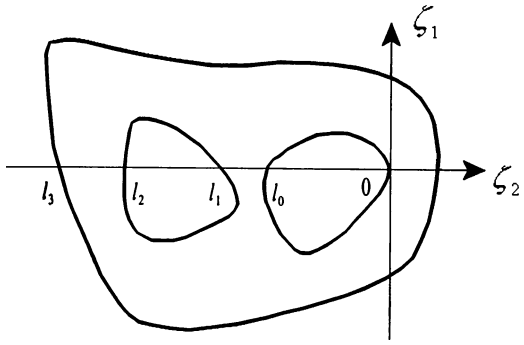

Fig. 4 Multiply connected domain.

The integrands in the transformed integrals do not present numerical difficulties for their evaluation, as they are at most weakly singular. Before the numerical implementation, however, the validity of the analytical transformation needs to be further examined. Consider, for example, the instance when the source point is on that part of the boundary at which the negative ζ_1 axis, the default branch cut of the multiple-valued function $\log(z)$, intersects the domain as shown in Fig. 2. The discontinuity along the branch cut will invalidate the application of the Green's theorem above if the domain is a simply connected convex region as shown in the figure. This problem can be easily resolved by redefining the argument range of z, $arg(z)$, as $0 < arg(z) \le 2\pi$ for all source points located along the side ABC. By this argument redefinition, the branch cut is actually reset to the positive ζ_1 axis. However, this argument redefinition cannot be used to overcome the discontinuity problem of the $\log(z)$ term in the integrands for a simply connected nonconvex domain such as the one schematically depicted in Fig. 3.

It is obvious that along the concave segment AB the discontinuity problem cannot be resolved, irrespective of whether the negative or the positive ζ_1 axis is chosen as the branch cut. As proposed by Zhang et al.,[12] if the outward normal n at an arbitrary source point is not directed toward any part of the domain, this difficulty can be easily overcome by redefining the principal value of $arg(z)$ to be

$$(\beta - 2\pi) < arg(z) \le \beta \tag{19}$$

It is also evident that this argument redefinition technique cannot always be applied to treat a simply connected domain with an arbitrary shape or even a multiply connected region intersected by the negative ζ_1 axis at (l_0, l_1) and (l_2, l_3) as shown in Fig. 4.

To resolve this problem, an infinitesimal strip of the domain about the discontinuity along the branch cut is removed, and the usual

limiting process to restore this strip is followed, as described in Zhang et al.[13] for body-force loading. For a general multiply connected domain intersected by the negative ζ_1 axis m times in the intervals (l_{2m-1}, l_{2m-2}), $(l_{2m-3}, l_{2m-3}), \ldots (l_1, l_0)$, the complete BIE for plane anisotropic thermoelasticity can be shown to have the following form:

$$C_{ij}u_i(P) + \int_S u_i(Q)T_{ij}(P, Q)\,\mathrm{d}S = \int_S t_i(Q)U_{ij}(P, Q)\,\mathrm{d}S + \int_S \gamma_{ik}n_k\Theta U_{ij}(P, Q)\,\mathrm{d}S + \int_{\hat{S}} [(\gamma_{i\underline{k}}\underline{Q}_{ijk,\underline{t}}\Theta - \gamma_{i\underline{k}}\underline{Q}_{ijk}\Theta_{,\underline{t}} + C_1\gamma_{i\underline{k}}\underline{R}_{ijk\underline{t}})n_{\underline{t}} - \gamma_{i\underline{k}}\underline{U}_{ij}(P, Q)\Theta n_k]\,\mathrm{d}\hat{S} + \sum_{n=1}^{m}\int_{l_{2n-1}}^{l_{2n-2}} L_j(\zeta_1)\,\mathrm{d}\zeta_1 \tag{20}$$

where the integrand $L_j(\zeta_1)$ for the extra line integral is given by

$$L_j(\zeta_1) = 4\pi\Theta\gamma_{i\underline{k}}\frac{K_{12}}{K_{11}}\mathrm{Im}\left\{\frac{r_{i1}A_{j1}\mu_{\underline{11}}\mu_{\underline{k1}}}{\mu_{\underline{11}}^2+\mu_{\underline{21}}^2} + \frac{r_{i2}A_{j2}\mu_{\underline{12}}\mu_{\underline{k2}}}{\mu_{\underline{12}}^2+\mu_{\underline{22}}^2}\right\} + 4\pi\Theta\gamma_{i\underline{k}}\frac{\sqrt{\Delta}}{K_{11}}\mathrm{Im}\left\{\frac{r_{i1}A_{j1}\mu_{\underline{21}}\mu_{\underline{k1}}}{\mu_{\underline{11}}^2+\mu_{\underline{21}}^2} + \frac{r_{i2}A_{j2}\mu_{\underline{22}}\mu_{\underline{k2}}}{\mu_{\underline{12}}^2+\mu_{\underline{22}}^2}\right\} - 4\pi\gamma_{i\underline{k}}\left(\frac{K_{12}}{K_{11}}\Theta_{,\underline{1}} + \frac{\sqrt{\Delta}}{K_{11}}\Theta_{,\underline{2}}\right)\zeta_1\mathrm{Im}\left\{\frac{r_{i1}A_{j1}\mu_{k1}}{\mu_{\underline{11}}^2+\mu_{\underline{21}}^2} + \frac{r_{i2}A_{j2}\mu_{k2}}{\mu_{\underline{12}}^2+\mu_{\underline{22}}^2}\right\} + C_1\pi\zeta_1^2\gamma_{i\underline{k}}\left(\frac{K_{12}}{K_{11}}\mathrm{Im}\left\{\frac{r_{i1}A_{j1}\mu_{\underline{k1}}}{\mu_{\underline{11}}\left(\mu_{\underline{11}}^2+\mu_{\underline{21}}^2\right)} + \frac{r_{i2}A_{j2}\mu_{\underline{k2}}}{\mu_{\underline{12}}\left(\mu_{\underline{12}}^2+\mu_{\underline{22}}^2\right)}\right\} + \frac{\sqrt{\Delta}}{K_{11}}\mathrm{Im}\left\{\frac{r_{i1}A_{j1}\mu_{\underline{k1}}}{\mu_{\underline{21}}\left(\mu_{\underline{11}}^2+\mu_{\underline{21}}^2\right)} + \frac{r_{i2}A_{j2}\mu_{\underline{k2}}}{\mu_{\underline{22}}\left(\mu_{\underline{12}}^2+\mu_{\underline{22}}^2\right)}\right\}\right) - 4\pi\Theta\left(\frac{K_{12}}{K_{11}}\gamma_{i\underline{1}} + \frac{\sqrt{\Delta}}{k_{11}}\gamma_{i\underline{2}}\right)\mathrm{Im}\{r_{i1}A_{j1} + r_{i2}A_{j2}\} \tag{21}$$

With all discontinuities removed from the domain, Eq. (20) is thus analytically exact for any physical domain. It can be solved for the boundary unknowns in the usual manner in conventional BEM analysis. The numerical evaluation of the extra surface integrals with the integrand of Eq. (21) presents no serious difficulty per se. However, it requires the temperature field data, including the temperature gradients, at all integration points along the negative ζ_1 axis for each source point along the boundary if this axis cuts through the domain. This process can be quite cumbersome in practice when the associated thermal field problem is to be treated separately. Now, the reasons why we treat the thermoelasticity problem in the sequentially coupled manner are obvious because not only the exact volume-to-surface integral transformation requires the direct domain mapping for the associated field problem as well, but also the temperature calculations at interior points might need to be carried out, although their coordinates will not be known until the collocation process for evaluating the transformed thermoelasticity BIE is performed.

To enable exact transformation of the volume integral, such a sequentially coupled treatment of thermoelasticity, therefore, necessitates the employment of the direct domain mapping for solving the associated field problem. To apply this approach in the sequentially coupled manner, the BEM codes for solving both problems—the anisotropic thermoelasticity and the associated thermal field—are integrated altogether into the same computer program as a single algorithm using the same mesh discretization of the boundary to facilitate such a sequentially coupled calculation. In the domain mapping process, however, the physical domain becomes distorted in the mapped plane. When a domain consists of several anisotropic regions, for each of which a different set of anisotropic coefficients are involved, the interfaces between the dissimilar conjoint materials will, in general, overlap or separate in the mapped plane as shown in Fig. 5. Although the mapped domain can be treated as an "isotropic" one, this overlapping or separation of interfaces, however, will invalidate the use of the compatibility equation for the temperature field in isotropic media when the conventional subregioning technique in BEM is employed. In what follows, the proper interfacial conditions, including the compatibility and the equilibrium equations, to treat the overlapping or separating interfaces between dissimilar subregions in the mapped plane will be investigated next.

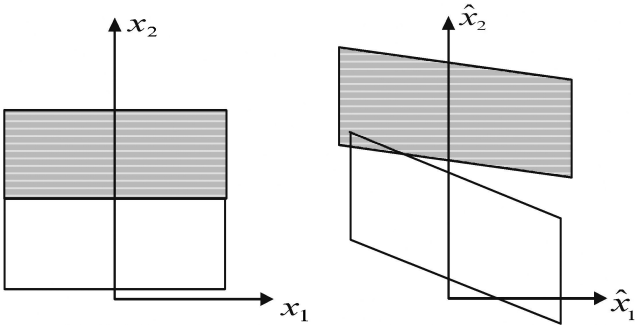

Fig. 5 Interfaces between dissimilar anisotropic media.

III. Interfacial Field Conditions in the Mapped Plane

As aforementioned, dealing with the associated temperature field is considered an integrated part of the intercoupled treatment of the anisotropic thermoelasticity in BEM. Although considered isotropic in the mapped plane, the distorted subregions of dissimilar anisotropic media can, in general, have overlapping or separating interfaces that would invalidate the use of the interfacial conditions in the conventional BEM subregioning technique for isotropic field problems. Because the temperature values at corresponding points in the mapped plane must remain identical with those in the physical plane, the values of temperature change at interfacial points, although not at the same mapped coordinates for dissimilar conjoint materials, must be identical from the equilibrium sense, that is,

$$\Theta^{(1)} = \Theta^{(2)} \tag{22}$$

where the superscript i is consistently used throughout this paper for denoting material i. However, because of the distortion of boundaries that results in misalignment of the unit outward normal vectors along the interfaces of adjacent materials, denoted by $n^{(1)}$ and $n^{(2)}$, the compatibility condition of heat fluxes needs to be reformulated accordingly. For this purpose, consider first the heat fluxes out of the interfaces between adjacent materials 1 and 2 in the physical plane, denoted by $Q_i^{(1)}$ and $Q_i^{(2)}$, respectively. The thermal compatibility between the interfaces of both materials requires that the sum of the normal heat fluxes across the interfaces shall vanish, that is,

$$Q_i^{(1)}n_i^{(1)} + Q_i^{(2)}n_i^{(2)} = 0 \tag{23}$$

which, for anisotropic materials, can be rewritten as

$$K_{ij}^{(1)}\Theta_{,j}^{(1)}n_i^{(1)} + K_{ij}^{(2)}\Theta_{,j}^{(2)}n_i^{(2)} = 0 \tag{24}$$

Expanding the preceding indicial expression will yield

$$\left(K_{11}^{(1)}\Theta_{,1}^{(1)} + K_{12}^{(1)}\Theta_{,2}^{(1)}\right)n_1^{(1)} + \left(K_{21}^{(1)}\Theta_{,1}^{(1)} + K_{22}^{(1)}\Theta_{,2}^{(1)}\right)n_2^{(1)} + \left(K_{11}^{(2)}\Theta_{,1}^{(2)} + K_{12}^{(2)}\Theta_{,2}^{(2)}\right)n_1^{(2)} + \left(K_{21}^{(2)}\Theta_{,1}^{(2)} + K_{22}^{(2)}\Theta_{,2}^{(2)}\right)n_2^{(2)} = 0 \tag{25}$$

By means of the chain rule to express the potential gradients in the new coordinate system $(\hat{x}_1, \hat{x}_2)$, Eq. (25) can be rewritten as

$$\Theta_{,\underline{1}}^{(1)}\sqrt{\Delta^{(1)}}\,n_1^{(1)} + \left[\frac{\left(\Theta_{,\underline{1}}^{(1)}\sqrt{\Delta^{(1)}} - \Theta_{,\underline{2}}^{(1)}K_{12}^{(1)}\right)K_{12}^{(1)}}{K_{11}^{(1)} + \Theta_{,\underline{2}}^{(1)}K_{22}^{(1)}}\right]n_2^{(1)}$$
$$+ \Theta_{,\underline{1}}^{(2)}\sqrt{\Delta^{(2)}}\,n_1^{(2)} + \left[\frac{\left(\Theta_{,\underline{1}}^{(2)}\sqrt{\Delta^{(2)}} - \Theta_{,\underline{2}}^{(2)}K_{12}^{(2)}\right)K_{12}^{(2)}}{K_{11}^{(2)} + \Theta_{,\underline{2}}^{(2)}K_{22}^{(2)}}\right]n_2^{(2)} = 0 \tag{26}$$

From the transformation matrix in Eq. (7), it can be readily proved that the unit outward normal vectors along the boundary in the physical plane can be written in terms of those in the mapped plane as

$$n_1 = \left(\hat{n}_1\sqrt{\Delta}\big/K_{11} - \hat{n}_2K_{12}/K_{11}\right)\big/\omega, \qquad n_2 = \hat{n}_2/\omega \tag{27}$$

where ω is given by

$$\omega = \sqrt{\left[\hat{n}_1\left(\sqrt{\Delta}\big/K_{11}\right) - \hat{n}_2(K_{12}/K_{11})\right]^2 + \hat{n}_2^2} \tag{28}$$

By substituting the expressions for n_1 and n_2, given by Eq. (27), into Eq (26), one can obtain a simple but important thermal compatibility equation, derived as follows:

$$\Theta_{,\underline{1}}^{(1)}\sqrt{\Delta^{(1)}}\left(\frac{\hat{n}_1^{(1)}\sqrt{\Delta^{(1)}} - \hat{n}_2^{(1)}K_{12}^{(1)}}{\omega^{(1)}K_{11}^{(1)}}\right)$$
$$+ \left(\frac{K_{12}^{(1)}\Theta_{,\underline{1}}^{(1)}\sqrt{\Delta^{(1)}} + \Delta^{(1)}\Theta_{,\underline{2}}^{(1)}}{\omega^{(1)}K_{11}^{(1)}}\right)n_2^{(1)}$$
$$+ \Theta_{,\underline{1}}^{(2)}\sqrt{\Delta^{(2)}}\left(\frac{\hat{n}_1^{(2)}\sqrt{\Delta^{(2)}} - \hat{n}_2^{(2)}K_{12}^{(2)}}{\omega^{(2)}K_{11}^{(2)}}\right)$$
$$+ \left(\frac{K_{12}^{(2)}\Theta_{,\underline{1}}^{(2)}\sqrt{\Delta^{(2)}} + \Delta^{(2)}\Theta_{,\underline{2}}^{(2)}}{\omega^{(2)}K_{11}^{(2)}}\right)n_2^{(2)}$$
$$= \frac{\Delta^{(1)}}{\omega^{(1)}K_{11}^{(1)}}\left(\Theta_{,\underline{1}}^{(1)}\hat{n}_1^{(1)} + \Theta_{,\underline{2}}^{(1)}\hat{n}_2^{(1)}\right)$$
$$+ \frac{\Delta^{(2)}}{\omega^{(2)}K_{11}^{(2)}}\left(\Theta_{,\underline{1}}^{(2)}\hat{n}_1^{(2)} + \Theta_{,\underline{2}}^{(2)}\hat{n}_2^{(2)}\right)$$
$$= \frac{\Delta^{(1)}}{\omega^{(1)}K_{11}^{(1)}}\frac{\mathrm{d}\Theta^{(1)}}{\mathrm{d}\hat{n}^{(1)}} + \frac{\Delta^{(2)}}{\omega^{(2)}K_{11}^{(2)}}\frac{\mathrm{d}\Theta^{(2)}}{\mathrm{d}\hat{n}^{(2)}} = 0 \tag{29}$$

By specifying the equilibrium and compatibility conditions according to Eqs. (22) and (29) for the interfaces between adjacent materials, the conventional subregioning technique in BEM can now be applied to simultaneously solve the BIE, Eq. (9), formulated for both materials. This subregioning process to solve the BIE for nodal unknowns along the boundary is well established in the BEM literature, and therefore it will not be elaborated herein. After the thermal field, including the temperature and its spatial gradients to the first order, is obtained for all boundary nodes, the sequentially coupled approach to solve the anisotropic thermoelasticity BIE as described earlier can then be applied to determine the thermal stresses along the boundary and interfaces. To illustrate the veracity and the applicability of the proposed scheme to treat the interfacial thermal stresses between dissimilar anisotropic materials, three numerical examples are presented with verifications by the analysis of ANSYS, commercial software based on the finite element method.

IV. Numerical Examples

As aforementioned, to facilitate the exact volume-to-surface integral transformation, the associated heat conduction and the thermoelasticity problem are treated in a sequentially coupled manner that shall demand amalgamation of both BEM programs, designed respectively for the both problems at first. The proposed BEM approach to treat the interfacial thermal stresses between dissimilar anisotropic composite materials has been implemented into our existing BEM computer codes based on the quadratic isoparametric element formulation. As illustrations to demonstrate the applicability and the ease of modeling such problems by the proposed approach, three example problems are investigated so that a composite structure consisting of multiple anisotropic materials is subjected to thermal loading.

The study for all examples shall investigate the interfacial thermal stresses of dissimilar anisotropic materials under the plane strain condition. Because of the difficulties we encountered in finding all necessary anisotropic constants, including all mechanical properties, thermal expansion coefficients, and conductivity coefficients, for some real materials in engineering use nowadays, simply for the demonstrative purpose, our analyses adopted the following arbitrarily chosen properties (Table 1) using the usual notations but with asterisks denoting values in the directions of the principal axes.

For verifications of the obtained results, all three problems are also solved by ANSYS6.0, commercial software based on the finite element method.

A. Example 1

As schematically depicted in Fig. 6, the first problem considered is a square block (material 1) in which a core column (material 2) is embedded. Principally, the example is to show the involvement of the extra surface integrals, formulated in Eqs. (20) and (21). Because material 1 is a multiply connected domain, the source nodes on its inner surface shall require the extra surface integrals to validate the integral transformation. As shown in Fig. 6, sides AB and CD are fixed and prescribed with $\Theta = 100$ deg, while the other two surfaces are insulated and free to move in any direction. Materials' principal axes are arbitrarily chosen to be oriented with 30 and 45 deg counterclockwise, respectively, for materials 1 and 2 to illustrate the applicability of the proposed scheme in accounting for full anisotropy. Also shown in Fig. 6 is the BEM mesh modeling of the boundary that uses 96 quadratic isoparametric elements with a total of 192 nodes. By applying the interfacial conditions, Eqs. (22) and (29), to the conventional subregioning technique for isotropic media in the mapped plane, the associated anisotropic heat-conduction problem is first solved to obtain the temperature and its spatial gradients at all boundary nodes. For evaluations of the extra surface

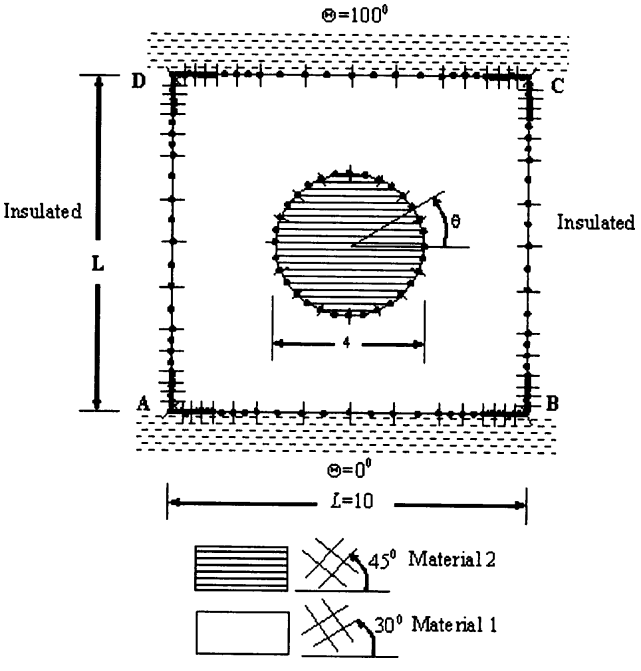

Fig. 6 Composite structure and its BEM meshes for problem 1.

Table 1 Material properties of the anisotropic materials

Material	E^*_{22}/E^*_{11}	E^*_{33}/E^*_{11}	G^*_{12}/E^*_{11}	G^*_{23}/E^*_{11}	G^*_{31}/E^*_{11}	$\alpha^*_{22}/\alpha^*_{11}$	ν^*_{12}	ν^*_{13}	ν^*_{23}	$\eta^*_{12,1}$	$\eta^*_{12,2}$	$\eta^*_{12,3}$	K^*_{22}/K^*_{11}
1	21/55	16/55	9.7/55	62/55	85/55	20/6.3	0.25	0.27	0.19	0	0	0	0.35/3.46
2	51.6/34.5	25/34.5	3.7/34.5	54/34.5	63/34.5	9/2.8	0.28	0.34	0.28	0	0	0	4.98/4.18
3	32.6/26.5	18.2/26.5	2.5/26.5	22.5/26.5	43.2/26.5	2.4/4.5	0.22	0.25	0.17	0	0	0	6.65/9.24

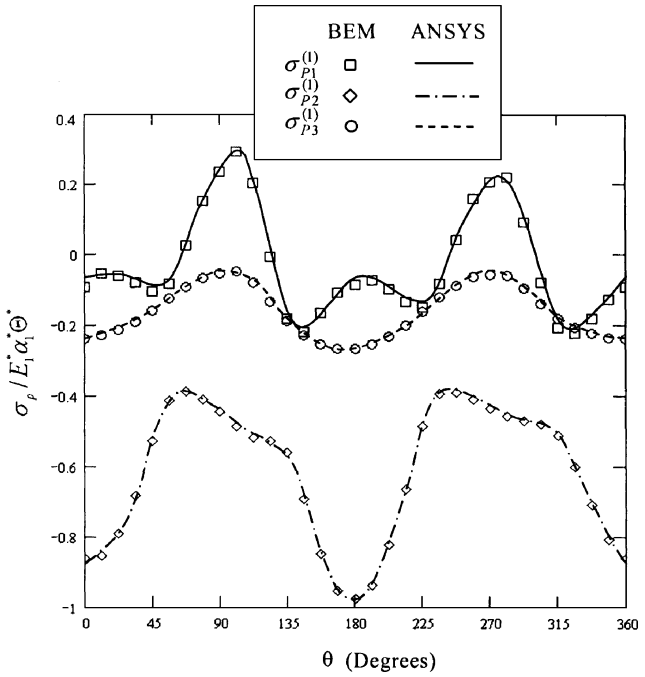

Fig. 7 Normalized principal stresses $\sigma^{(1)}_P/E^*_{11}\alpha^*_{11}\Theta^*$ along the interface of material 1: problem 1.

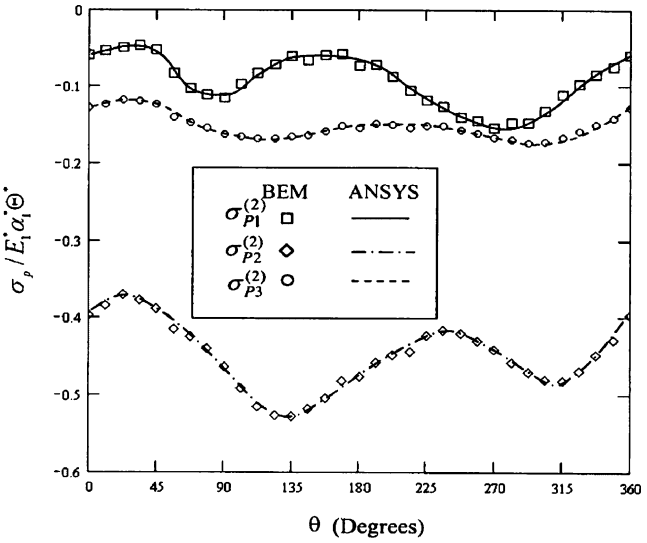

Fig. 8 Normalized principal stresses $\sigma^{(2)}_P/E^*_{11}\alpha^*_{11}\Theta^*$ along the interface of material 2: problem 1.

integrals with source points of material 1 lying along the circumference of the hole, the required temperature data at interior Gauss integration points are interactively calculated using the BEM codes for the associated heat-conduction problem while the thermoelasticity boundary integral equation is still being solved. As is obvious, the involvement of the extra surface integrals for this example has indeed highlighted the nature of such an inter-coupled treatment. For verification of the BEM result, the problem is also solved by ANSYS6.0 with 3712 PLANE-42 elements applied for the domain discretization. The calculated principal stresses along the interfaces, $\sigma^{(i)}_{p1}$, $\sigma^{(i)}_{p2}$, and $\sigma^{(i)}_{p3}$ with the superscript i denoting the material i, are normalized by $E^*_{11}\alpha^*_{11}\Theta^*(\Theta^* = 100$ deg) and plotted in Figs. 7 and 8 for material 1 and 2, respectively. As can be observed from the comparison of both results shown in the figures, excellent agreement has shown the veracity of the proposed BEM approach.

B. Example 2

As an illustration to demonstrate the applicability of the proposed BEM scheme, the second example is to consider a laminated composite structure, consisting of four layers of anisotropic materials (materials 1 and 2) symmetrically piling up as schematically depicted in Fig. 9. The material principal axes are assumed to have a different orientation for each layer as illustrated in the figure. As the boundary conditions of the associated heat-conduction problem, sides EG and FH are, respectively, prescribed with a temperature change $\Theta = 0$ and 100 deg, whereas the other two opposite surfaces are thermally insulated. Suppose that the insulated surfaces, EF and GH, are constrained, and the other two sides are completely free to move in any direction. Because of the characteristic of symmetry, our analyses are carried out only for the lower half part, as shown in Fig. 10. Also shown is the BEM mesh discretization, where only 92 quadratic isoparametric elements with a total of 184 nodes are applied over the boundary. The FEM modeling for the ANSYS analysis

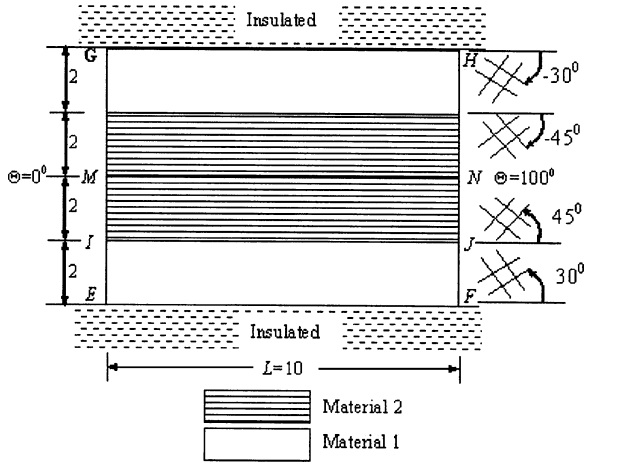

Fig. 9 Layered composite structure subjected to thermal loading: problem 2.

involves 2048 PLANE-42 elements. In a similar manner as in the preceding example, the calculated principal stresses along the interfaces are normalized by the same factor $E^*_{11}\alpha^*_{11}\Theta^*(\Theta^* = 100$ deg). To visualize the variations of the normalized principal stresses along all interfaces, the values are plotted as a function of the nondimensional distance x_1/L in Figs. 11–13 for the interface $IJ^{(1)}$, $IJ^{(2)}$, and MN, respectively. Again, excellent agreements between the results obtained by the proposed BEM approach and FEM can be seen from such comparison shown in these figures.

C. Example 3

To show the applicability of the proposed BEM scheme for a somewhat more complicated case, the last example problem considers a composite structure consisting of three different anisotropic materials with intersecting interfaces as shown in Fig. 14. The materials' principal axes are arbitrarily chosen to be oriented with 30, 45, and 60 deg measured counterclockwise from the x_1 axis for materials

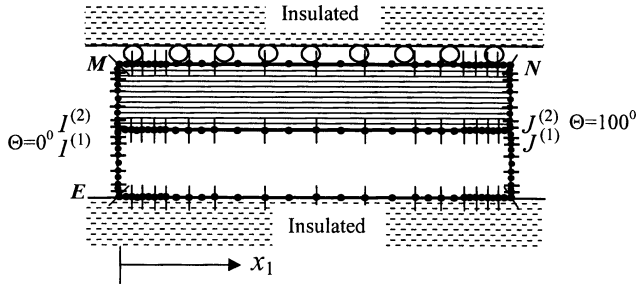

Fig. 10 BEM modeling and its mesh discretisation for problem 2.

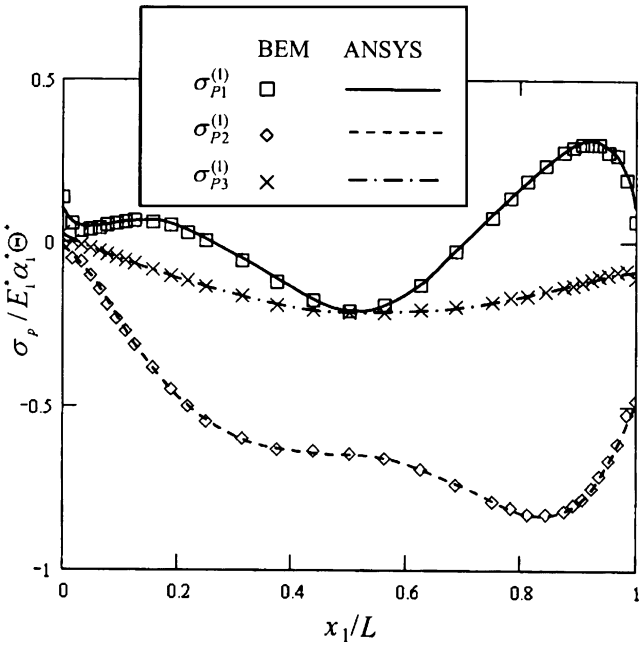

Fig. 11 Normalized principal stresses $\sigma_p/E_1^*\alpha_1^*\Theta^*$ along the interface $IJ^{(1)}$: problem 2.

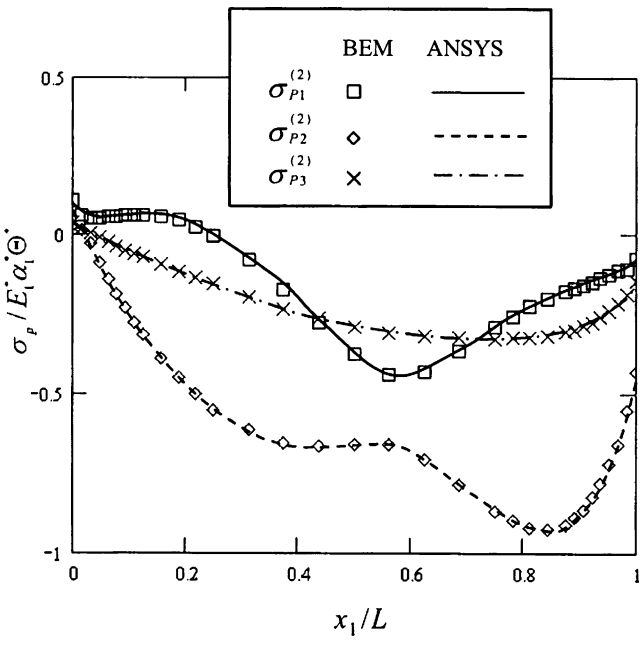

Fig. 12 Normalized principal stresses $\sigma_p/E_1^*\alpha_1^*\Theta^*$ along the interface $IJ^{(2)}$: problem 2.

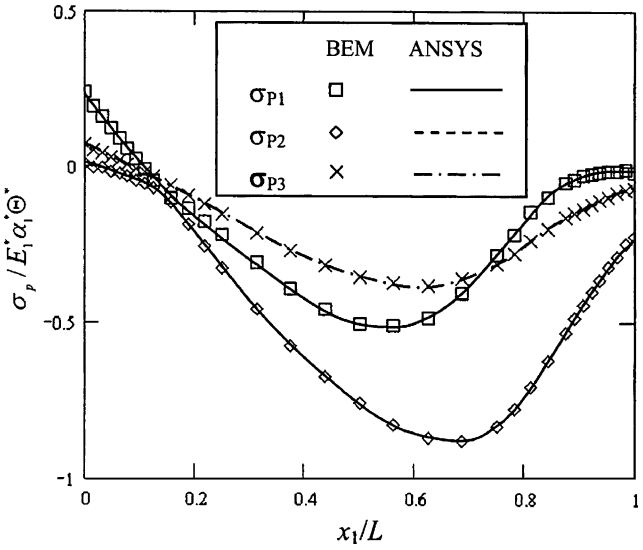

Fig. 13 Normalized principal stresses $\sigma_p/E_1^*\alpha_1^*\Theta^*$ along the interface MN: problem 2.

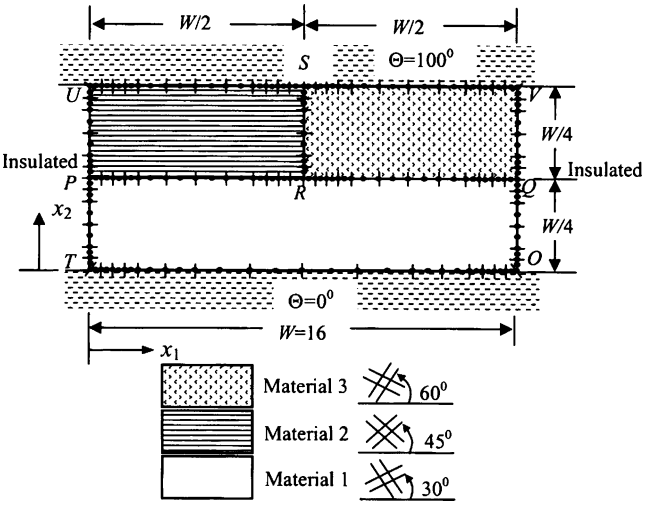

Fig. 14 Composite structure subjected to thermal loading and its BEM meshes: problem 3.

1, 2, and 3, respectively. Suppose that the boundaries TO and UV are, respectively, subjected to a temperature change $\Theta = 0$ and 100 deg, while the other two opposite surfaces are thermally insulated. As the prescribed boundary conditions, sides TO and UV are constrained, and the other two surfaces are free to move in any direction. For the BEM approach, the associated heat-conduction problem is first solved by applying the interfacial conditions, Eqs. (22) and (29), for all interfaces between any two adjacent materials. In proceeding to solve the associated thermoelasticity boundary integral equation, the same distorted mesh data are used for evaluation of the transformed integrals in the mapped plane. Also shown in Fig. 14 is the BEM mesh discretization that only 124 quadratic isoparametric elements with a total of 248 nodes are applied to model the whole boundaries. For the FEM mesh discretization in ANSYS, a total of 2048 PLANE-42 elements are applied to model the whole domain. The principal stresses along the interface PQ of all materials calculated by both schemes are normalized by the same factor as in the preceding examples. Figure 15 shows the normalized principal stresses along the interface PQ on material 1, whereas the normalized values for materials 2 and 3 are shown in Fig. 16. As expected, there is a jump of the principal stresses across materials 2 and 3 as a result of the conjoint of dissimilar materials. The normalized principal stresses along RS are plotted in Figs. 17 and 18 as a function of the nondimensional distance x_2/W along the interface on materials

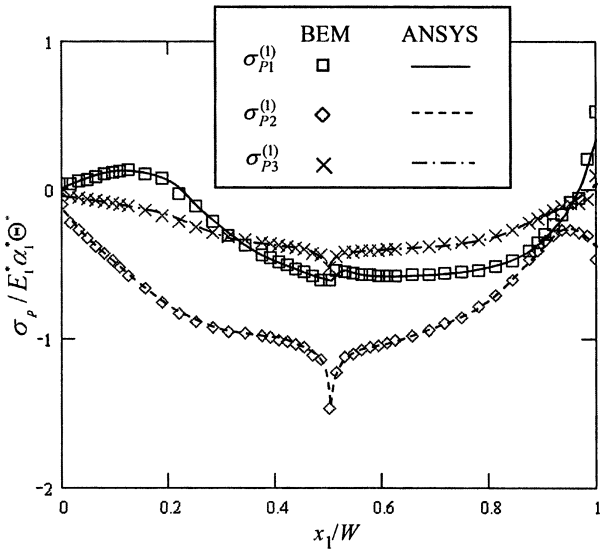

Fig. 15 Normalized principal stresses $\sigma_P^{(1)}/E_1^*\alpha_1^*\Theta^*$ along the interface $PQ^{(1)}$: problem 3.

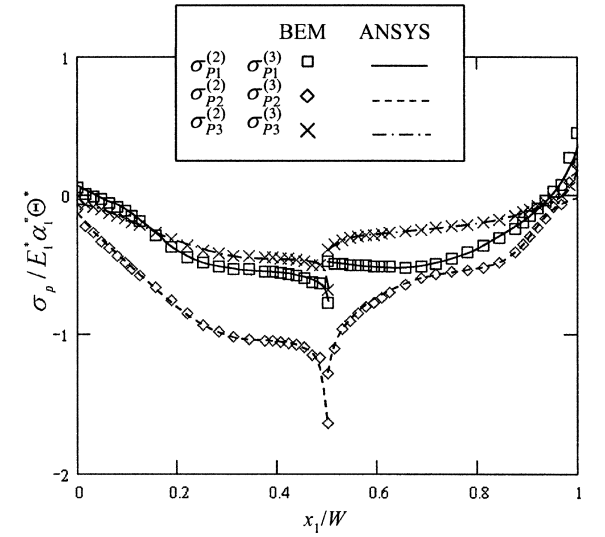

Fig. 16 Normalized principal stresses $\sigma_P^{(2)}/E_1^*\alpha_1^*\Theta^*$ and $\sigma_P^{(3)}/E_1^*\alpha_1^*\Theta^*$ along the interfaces $PQ^{(2)}$ and $PQ^{(3)}$: problem 3.

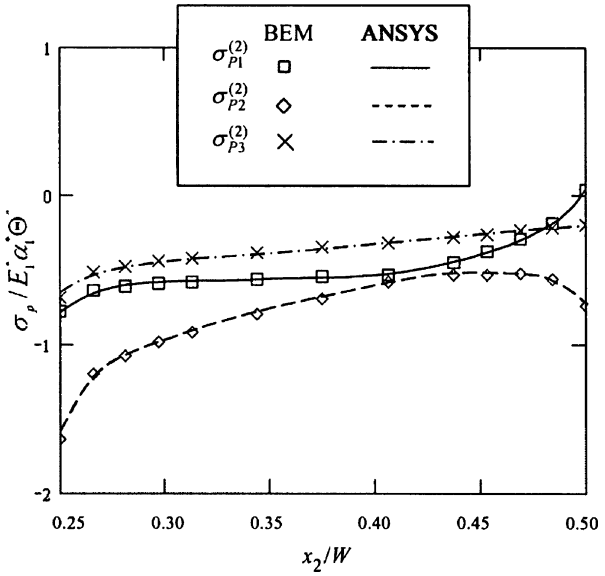

Fig. 17 Normalized principal stresses $\sigma_P^{(2)}/E_1^*\alpha_1^*\Theta^*$ along the interface $RS^{(2)}$: problem 3.

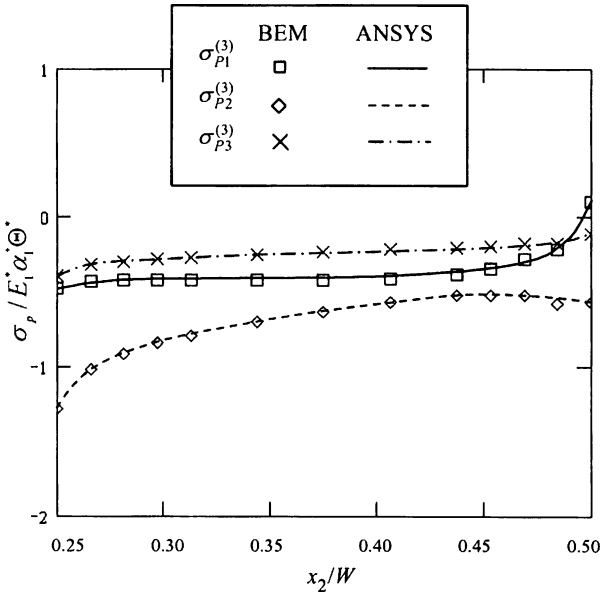

Fig. 18 Normalized principal stresses $\sigma_P^{(3)}/E_1^*\alpha_1^*\Theta^*$ along the interface $RS^{(3)}$: problem 3.

2 and 3, respectively. As can be seen from the comparison of results shown in these figures, excellent agreements of the obtained results have once again confirmed the validity of the proposed BEM approach.

V. Conclusions

Boundary-element-method (BEM) researches on the interfacial thermal stresses between generally anisotropic materials that are subjected to general thermal loading still remain unexplored in the literature. The present work applies an intercoupled treatment in conjunction with the conventional subregioning technique in BEM to deal with the problem. The proposed approach is featured by its generality in accounting for materials' full anisotropies, coupled with general thermal fields. For this approach, such evaluation of the transformed integrals would, however, generally require interactive calculations of all temperature and its spatial gradients at all integration points. Unlike other BEM schemes that are commonly adopted for such analysis, the proposed scheme has the merit that both the thermal field and the elasticity problems are solved altogether using the same mesh discretization, and no further numerical approximation is incurred. Especially, such interactive calculations are necessary for a multiply connected region that shall involve field calculations at interior points. As compared with other BEM schemes, it is apparent that such an approach has restored BEM's spirit as a truly boundary solution technique for the general thermoelasticity problem of multiply bonded anisotropic composites.

Acknowledgments

The authors gratefully acknowledge the financial support by the National Science Council of Taiwan, Republic of China (Grants NSC-92-2212-E-035-012 and NSC-93-2212-E-035-006).

References

[1]Suhir, E., "Interfacial Stresses in Bi-Metal Thermostats," *Journal of Applied Mechanics*, Vol. 56, March 1989, pp. 595–600.

[2]Yin, W. L., "Interfacial Thermal Stresses in Layered Structures: the Stepped Problem," *Journal of Electronic Packaging*, Vol. 117, No. 2, 1995, pp. 153–158.

[3]Camp, C. V., and Gipson, G. S., *Boundary Element Analysis of Nonhomogeneous Biharmonic Phenomena*, Springer-Verlag, Berlin, 1992, pp. 135–156.

[4]Lachat, J. C., "Further Development of the Boundary Integral Technique for Elastostatics," Ph.D. Dissertation, Dept. of Civil Engineering and the Environment, Southampton Univ., Southampton, England, U.K., May 1975.

[5]Deb, A., and Banerjee, P. K., "BEM for General Anisotropic 2D Elasticity Using Particular Integrals," *Communications in Applied Numerical Methods*, Vol. 6, No. 2, 1990, pp. 111–119.

[6]Rizzo, F. L., and Shippy, D. J., "An Advanced Boundary Integral Equation Method for Three-Dimensional Thermoelasticity," *International Journal for Numerical Methods in Engineering*, Vol. 11, No. 11, 1977, pp. 1753–1768.

[7]Tan, C. L., "Boundary Integral Equation Stress Analysis of a Rotating Disc with Corner Crack," *Journal of Strain Analysis*, Vol. 18, No. 4, 1983, pp. 231–237.

[8]Danson, D., "Linear Isotropic Elasticity with Body Forces," *Progress in Boundary Element Methods*, edited by C. A. Brebbia, Pentech Press, London, 1983, pp. 247–258.

[9]Shiah, Y. C., and Tan, C. L., "Exact Boundary Integral Transformation of the Thermoelastic Domain Integral in BEM for General 2D Anisotropic Elasticity," *Computational Mechanics*, Vol. 23, No. 1, 1999, pp. 87–96.

[10]Shiah, Y. C., and Tan, C. L., "Determination of Interior Point Stresses in Two-Dimensional BEM Thermoelastic Analysis of Anisotropic Bodies," *International Journal of Solids and Structures*, Vol. 37, No. 5, 2000, pp. 809–829.

[11]Shiah, Y. C., and Tan, C. L., "BEM Treatment of Two-Dimensional Anisotropic Field Problems by Direct Domain Mapping," *Engineering Analysis with Boundary Elements*, Vol. 20, No. 4, 1998, pp. 347–351.

[12]Zhang, J. J., Tan, C. L., and Afagh, F. F., "An Argument Redefinition Procedure in the BEM for 2D Anisotropic Elastostatics with Body Forces," *Proceedings of the Symposium on Mechanics in Design*, Vol. 1, edited by S. A. Meguid, 1996, pp. 349–358.

[13]Zhang, J. J., Tan, C. L., and Afagh, F. F., "A General Exact Transformation of Body-Force Volume Integral in BEM for 2D Anisotropic Elasticity," *Computational Mechanics*, Vol. 19, No. 1, 1996, pp. 1–10.

K. Shivakumar
Associate Editor